

Field-tunable Berezinskii-Kosterlitz-Thouless correlations in a Heisenberg magnet

D. Opherden,¹ M. S. J. Tepaske,^{2,3} F. Bärtl,^{1,4} M. Weber,³ M. M. Turnbull,⁵ T. Lancaster,⁶ S. J. Blundell,⁷ M. Baenitz,⁸ J. Wosnitza,^{1,4} C. P. Landee,⁹ R. Moessner,³ D. J. Luitz,^{2,3} and H. Kühne^{1,*}

¹*Hochfeld-Magnetlabor Dresden (HLD-EMFL) and Würzburg-Dresden Cluster of Excellence ct.qmat, Helmholtz-Zentrum Dresden-Rossendorf, 01328 Dresden, Germany*

²*Physikalisches Institut, Universität Bonn, Nussallee 12, 53115 Bonn, Germany*

³*Max Planck Institute for the Physics of Complex Systems, 01187 Dresden, Germany*

⁴*Institut für Festkörper- und Materialphysik, TU Dresden, 01062 Dresden, Germany*

⁵*Carlson School of Chemistry, Clark University, Worcester, MA 01610, USA*

⁶*Durham University, Centre for Materials Physics, South Road, Durham DH1 3LE, UK*

⁷*Clarendon Laboratory, Department of Physics, University of Oxford, Park Road, Oxford OX1 3PU, UK*

⁸*Max Planck Institute for Chemical Physics of Solids, 01187 Dresden, Germany*

⁹*Department of Physics, Clark University, Worcester, MA 01610, USA*

(Dated: September 23, 2022)

We report the manifestation of field-induced Berezinskii-Kosterlitz-Thouless (BKT) correlations in the weakly coupled spin-1/2 Heisenberg layers of the molecular-based bulk material $[\text{Cu}(\text{pz})_2(2\text{-HOpy})_2](\text{PF}_6)_2$. Due to the moderate intralayer exchange coupling of $J/k_B = 6.8$ K, the application of laboratory magnetic fields induces a substantial XY anisotropy of the spin correlations. Crucially, this provides a significant BKT regime, as the tiny interlayer exchange $J'/k_B \approx 1$ mK only induces 3D correlations upon close approach to the BKT transition with its exponential growth in the spin-correlation length. We employ nuclear magnetic resonance and μ^+ SR measurements to probe the spin correlations that determine the critical temperatures of the BKT transition as well as that of the onset of long-range order. Further, we perform stochastic series expansion quantum Monte Carlo simulations based on the experimentally determined model parameters. Finite-size scaling of the in-plane spin stiffness yields excellent agreement of critical temperatures between theory and experiment, providing clear evidence that the nonmonotonic magnetic phase diagram of $[\text{Cu}(\text{pz})_2(2\text{-HOpy})_2](\text{PF}_6)_2$ is determined by the field-tuned XY anisotropy and the concomitant BKT physics.

Cooperative behavior and critical phenomena of strongly correlated magnets are typically dictated by the lattice and spin dimensions, as well as by the symmetry of the underlying Hamiltonian [1–8]. Among the most fascinating examples are two-dimensional (2D) XY spin systems, which are known to undergo a topological Berezinskii-Kosterlitz-Thouless phase transition at a finite temperature T_{BKT} [9–11], which marks the binding of topological defects in vortex-antivortex pairs. So far, experimental efforts to probe a genuine BKT transition in a bulk material were compromised by the onset of 3D order [12–18] due to the inherent 3D nature of these materials. Still, if the perturbative terms relative to a purely 2D XY model are small enough, the experimental observation of magnetic properties associated with BKT correlations may be possible in the transition regime [19–22].

In particular, a controlled tuning of the XY anisotropy, with associated impact on T_{BKT} , can provide an ideal test bed for experimental studies of BKT physics and their comparison to numerical state-of-the-art modeling. As a possible approach to tune the magnetic correlations away from 2D Heisenberg to a 2D XY symmetry, the application of a uniform magnetic field to the 2D quantum Heisenberg antiferromagnet breaks the $O(3)$ symmetry, but preserves the easy-plane $O(2)$ symmetry, as was confirmed by quantum Monte Carlo (QMC) calculations [23]. Correspondingly, for Zeeman energies of the order of the exchange energy, the effective XY -exchange

anisotropy can be controlled. The associated BKT transition persists for all fields below saturation, yielding a nonmonotonic magnetic phase diagram [23].

In order to find materials which allow to study this phenomenology, the chemical engineering of molecular-based bulk magnets is a promising approach. By an appropriate choice of molecular ligands and counterions, the syntheses of several materials that realize a 2D spin-1/2 Heisenberg model on the square lattice were reported [24–34]. In these materials, a moderate nearest-neighbor exchange interaction of the order of a few K allows for the tunability of the effective exchange anisotropy by experimentally accessible magnetic fields. Indeed, for several Cu^{2+} -based molecular materials, a nonmonotonic magnetic phase diagram as a function of the external field was reported [24, 29, 31, 35, 36]. The magnetic properties of these molecular-based 2D quantum Heisenberg antiferromagnets were mostly investigated by thermodynamic methods [25, 29, 31, 33, 34], thus missing local information about the magnetic correlations in the BKT transition regime.

In this Letter, we report on the field-tunable anisotropy of magnetic correlations in $[\text{Cu}(\text{pz})_2(2\text{-HOpy})_2](\text{PF}_6)_2$ [with $\text{pz} = \text{C}_4\text{H}_4\text{N}_2$, $2\text{-HOpy} = \text{C}_5\text{H}_4\text{NHO}$] (CuPOF in the following), ranging from the almost-isotropic Heisenberg limit at zero field to a substantial XY anisotropy upon increasing the magnetic field strength. We use nuclear magnetic resonance (NMR), as well as muon spin

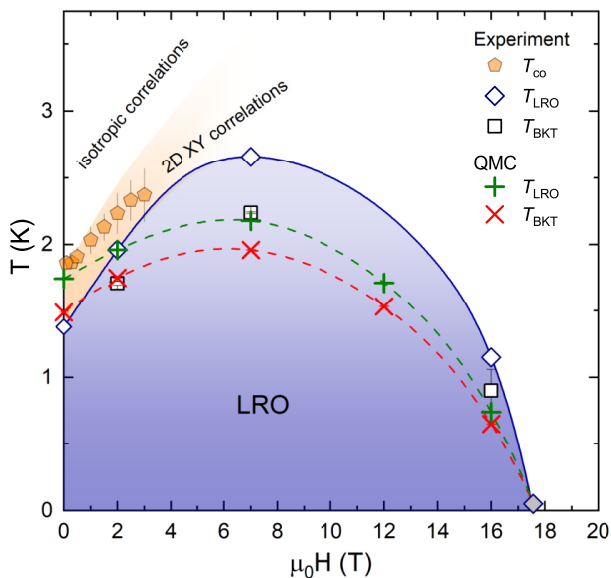


Figure 1. Phase diagram of CuPOF for out-of-plane magnetic fields from experiment and numerics. The pentagons denote the spin-anisotropy crossover temperature T_{co} from Ref. [24]. White diamonds indicate the transition temperature T_{LRO} to long-range order, and squares show the BKT transition temperature T_{BKT} , as obtained from the analysis of the ^{31}P $1/T_1$ rate (Fig. 2). T_{LRO} at zero field is determined by μ^+ SR measurements [24]. The green pluses and red crosses denote T_{LRO} and T_{BKT} , respectively, as obtained from QMC calculations (Fig. 3). The diamond at 17.5 T denotes the saturation field, which was determined from magnetization experiments [24], and is in agreement with QMC results. All lines are guides to the eye.

relaxation (μ^+ SR) as experimental probes for the dynamic and quasi-static spin correlations. Furthermore, by QMC simulations, we calculate the in-plane spin stiffness, which we use to determine the critical temperatures of the long-range order (LRO) and the BKT transition. Our main findings are (i) that the temperature dependence of the nuclear spin-lattice relaxation rate follows the behavior predicted from 2D BKT theory in a wide range of temperatures, determined by the field-driven anisotropy, (ii) that finite-size scaling of the QMC results permits the extraction of T_{BKT} , which lies below the actual 3D ordering temperature T_{LRO} , and (iii) that both temperatures exhibit a nonmonotonic field dependence, which is analogous to the behavior when instead of the field the anisotropy of interactions is tuned, a clear signature for the tunability of BKT correlations.

The synthesis and characterization of CuPOF by means of various techniques, including the μ^+ SR experiments, are described in Ref. [24]. The NMR spectra and spin-lattice relaxation time T_1 were recorded using a standard Hahn spin-echo pulse sequence and an inversion-recovery method, respectively. The measurements were performed using a commercial phase-

coherent spectrometer and a 16 T superconducting magnet, equipped with a ^3He sample-in-liquid cryostat.

The magnetic interactions of CuPOF in an applied field are well approximated by the effective Hamiltonian

$$\mathcal{H} = J \sum_{\langle i,j \rangle_{\parallel}} [S_i^x S_j^x + S_i^y S_j^y + (1 - \Delta) S_i^z S_j^z] + J' \sum_{\langle i,j \rangle_{\perp}} \mathbf{S}_i \cdot \mathbf{S}_j - g\mu_B \mu_0 H \sum_i S_i^z, \quad (1)$$

where $\langle i,j \rangle_{\parallel}$ and $\langle i,j \rangle_{\perp}$ denote the intra- and interlayer nearest-neighbors, and J and J' are the intra- and interlayer exchange couplings, estimated as $J/k_B = 6.8$ K and $J'/k_B \approx 1$ mK [24]. Whereas $\Delta = 0$ corresponds to the isotropic Heisenberg case, $0 < \Delta \leq 1$ quantifies an easy-plane anisotropy, with a zero-field value of $\Delta \approx 0.01 \dots 0.02$ for CuPOF [24].

In the presence of interlayer interactions, any non-frustrated magnetic quasi-2D lattice inevitably undergoes a transition to long-range order at low temperatures. Due to the very large separation of the magnetic layers in CuPOF, with $J'/J \approx 1.4 \cdot 10^{-4}$, the very small entropy change associated with the transition to LRO is beyond the experimental resolution of thermodynamic quantities [24, 37]. On the other hand, μ^+ SR is very sensitive to the local staggered magnetization, and was used to probe the transition to LRO at 1.38(2) K in CuPOF [24]. This transition occurs under the influence of the weak intrinsic easy-plane anisotropy, which yields a temperature-driven crossover from isotropic to XY -type correlations at the crossover temperature $T_{co} > T_{LRO}$. An applied magnetic field increases the effective XY anisotropy, which manifests itself as a field-dependent minimum of the uniform bulk susceptibility at T_{co} , as depicted by the pentagons in Fig. 1.

The temperature dependence of the ^{31}P -NMR spin-lattice relaxation rate at out-of-plane fields up to 16 T is presented in Figs. 2(a)–(c). The spin-lattice relaxation rate $1/T_1$ has sharp maxima at $T_{LRO} = 1.96$ and 2.66 K at 2 and 7 T, respectively. In comparison, the maximum amplitude of $1/T_1$ at 16 T ($T_{LRO} = 1.15$ K) is substantially reduced. The transition temperatures between the 2D XY and the LRO regimes are depicted by diamonds in Fig. 1. The strong dependence of T_{LRO} on the field strength that we observe in CuPOF clearly indicates a field-tunability of the XY anisotropy of the spin correlations [23]. This behavior is confirmed by our QMC simulations.

As previously reported, the ^{31}P $1/T_1$ rate in CuPOF yields several broad maxima at high temperatures, which are associated with a freezing of the PF_6 molecular reorientation modes [38]. Below about 10 K, in the range of interest in the present study, these modes are frozen out and $1/T_1$ becomes temperature independent, indicating predominantly paramagnetic fluctuations. In 2D magnetic lattices, the onset of short-range spin correlations

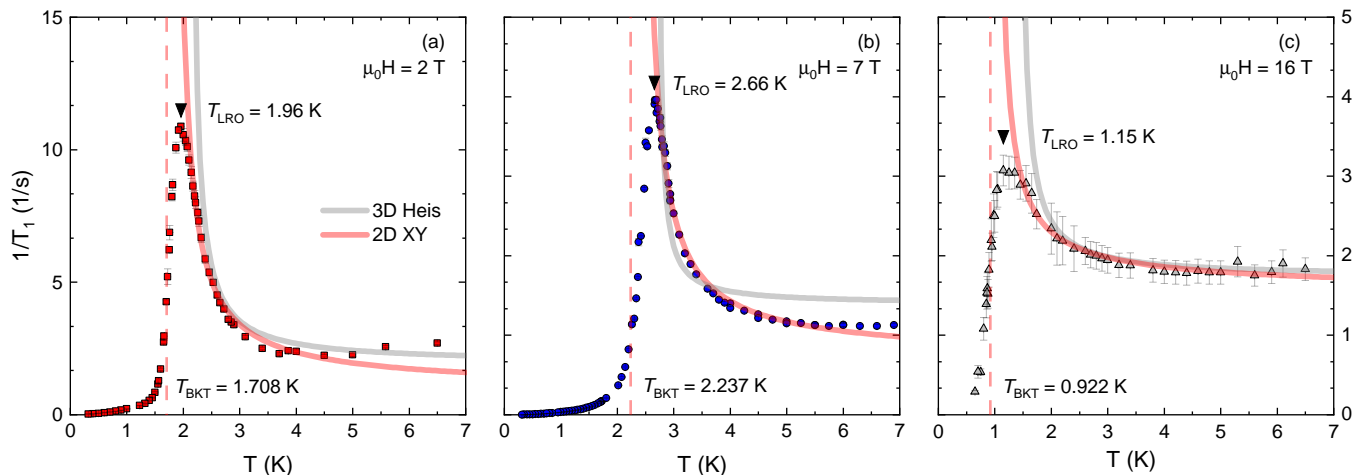


Figure 2. (a)–(c) Temperature-dependent ^{31}P nuclear spin-lattice relaxation rate $1/T_1$ of CuPOF, recorded at out-of-plane fields of 2, 7, and 16 T. The solid lines are best fits according to $1/T_1 \propto \xi^{z-\eta}$ for the temperature dependent correlation lengths $\xi_{3\text{DHeis}}$ and $\xi_{2\text{DXY}}$ of the 3D Heisenberg and the 2D XY cases (see main text). The transition temperature T_{LRO} , marked with a downward triangle, is inferred from the $1/T_1$ peak position, and T_{BKT} , marked with a dotted line, is determined from fits according to $1/T_1 \propto \xi_{2\text{DXY}}^{z-\eta}$. At all fields, but most noticeably at 7 T, $1/T_1$ is described best by $\xi_{2\text{DXY}}$ at $T \gtrsim T_{\text{LRO}}$.

occurs at temperatures $T \simeq J/k_B$ [37], with a correlation length of about one magnetic-lattice constant [16, 39].

At temperatures above the onset of LRO, $1/T_1$ can serve as a probe for the dynamic correlation length ξ [19, 20, 40–43]. As was shown from dynamical scaling arguments [40], $1/T_1$ is proportional to the transverse spin correlation length as $1/T_1 \propto \xi^{z-\eta}$, where z and η are characteristic dynamic and critical exponents [3, 19, 40, 44]. By comparing the temperature dependence of $1/T_1$ with the characteristic ξ of different universality classes, we can therefore probe the nature of the predominant correlations in the critical regime, before the system finally undergoes the transition to long-range order. Thus, we compare the BKT correlation length of a 2D easy-plane antiferromagnet, $\xi_{2\text{DXY}} \propto \exp(0.5\pi/\sqrt{T/T_{\text{BKT}} - 1})$ [11, 16], with that of a 3D isotropic Heisenberg antiferromagnet, $\xi_{3\text{DHeis}} \propto |T - T_{\text{LRO}}|^{-0.7112}$ [45, 46].

To describe $1/T_1$ in the interval $T_{\text{LRO}} \leq T \leq J/k_B$, we note that $\eta = 0.0375$ for the 3D Heisenberg antiferromagnet [45], with the LRO transition residing in the $O(3)$ universality class, whereas the easy-plane model has $\eta = 1/4$ [47–49]. For both models, we use $z = d/2$, with d the spatial dimensionality [44]. The experimental estimates of T_{BKT} are obtained from fits to the 2D XY form.

In Figs. 2(a)–(c), we show the measured $1/T_1$ along with both fits, for fields of 2, 7, and 16 T [50]. In contrast to the 3D Heisenberg description, the 2D XY fit accurately captures the increase of $1/T_1$ near T_{LRO} , most noticeably at 7 T. The fits yield $T_{\text{BKT}} = 1.708(14)$, $2.237(7)$, and $0.90(16)$ K for applied fields of 2, 7, and 16 T, respectively. The nonmonotonic dependence of T_{BKT} on

the field tracks that of T_{LRO} , being separated by a few hundred mK for the most part, as shown in the phase diagram in Fig. 1. One should note, however, that the BKT transition is preempted by the LRO that arises from the 3D correlations, stemming from the finite interlayer exchange interaction J' . In the supplemental material (SM) [52], we discuss indications that changing the field strength has similar effects on the spin correlations as changing the exchange anisotropy Δ [16, 51] and argue that hence the field allows to tune the effective anisotropy.

In order to shed more light on the experimentally observed phenomenology of mixed Néel and BKT-type correlations, we numerically investigate the Hamiltonian (1) using stochastic series expansion quantum Monte Carlo with directed loops [53]. We consider finite simple-cubic lattices with periodic boundary conditions and dimensions $L \times L \times L/8$, fixing $J/k_B = 6.8$ K, $J'/k_B = 1$ mK, and $\Delta = 0.0185$. To determine T_{BKT} and T_{LRO} , we calculate the in-plane spin stiffness $\rho = 8L^{-3} \partial^2 F / \partial \phi^2 \big|_{\phi=0}$, which is defined as the second derivative of the free energy F with respect to a uniform in-plane twist angle ϕ [54, 55]. This quantity is non-zero in the BKT phase and in the thermodynamic limit it should vanish instantly at T_{BKT} . For the finite lattices simulated with QMC, this drop-off is instead continuous, but based on how ρ approaches the instant drop-off with increasing system size, we can determine T_{BKT} . In particular, using finite-size scaling theory, it is predicted that ρ depends on temper-

ature T and system size L as [54]

$$\rho(T, L)/P(L) = f\left(\ln(L) - \frac{a}{\sqrt{T - T_{\text{BKT}}}}\right), \quad (2)$$

$$P(L) = 1 + \frac{1}{2\ln(L) + c + \ln[c/2 + \ln L]} + \frac{b}{\ln^2 L}, \quad (3)$$

where a, b, c are fitting constants and f is a general continuous function which we choose to be a fifth-order polynomial. This parameterization of ρ is fitted closely above T_{BKT} for simulation data of the $J' = 0$ model to deduce T_{BKT} . Afterwards, we plot ρ/P versus $\ln(L) - a/\sqrt{T - T_{\text{BKT}}}$ in the fitting interval, which should collapse to a single curve if the fit is perfect. We checked that fitting ρ for $J' = 1$ mK in the full 3D model reproduces the 2D T_{BKT} to within error bars, when fitted at $T > T_{\text{LRO}}$, where the interlayer coupling becomes insignificant such that the 2D scaling ansatz (3) holds. In Fig. 3(a), we show the finite-size collapse of the ρ fit performed at 2 T, for systems with up to one million spins and a temperature grid of $\Delta T = 1$ mK. The fit yields $T_{\text{BKT}} = 1.748(15)$ K.

To determine T_{LRO} , we consider the scaled in-plane stiffness $L\rho$ for the full 3D model with $J' = 1$ mK. At large L , this quantity becomes size independent at T_{LRO} [46]. Hence, by determining the crossings T^* between $L\rho$ curves with two different sizes L , and extrapolating this crossing temperature to $L \rightarrow \infty$, we obtain T_{LRO} [56]. In Fig. 3(b), we show the scaling analysis performed for $L\rho$ at 2 T, where the inset shows the $L \rightarrow \infty$ scaling of the crossing temperature T^* . Here, we used a second-order polynomial, which yields $T_{\text{LRO}} = 1.959(2)$ K. Further calculations of the relevant magnetization components and correlation length are presented in Fig. S3 of the SM [52].

Employing these procedures at different magnetic fields, we determined $T_{\text{BKT}} = 1.4877(6), 1.7477(15), 1.9584(24), 1.5323(13),$ and $0.6495(15)$ K, at fields of 0, 2, 7, 12, and 16 T, respectively. We also confirmed that $T_{\text{BKT}} = 0$ when both $\Delta = 0$ and $H = 0$, which emphasizes the strong effect on T_{BKT} of the seemingly small $\Delta = 0.0185$ for CuPOF. Furthermore, we determined $T_{\text{LRO}} = 1.7425(19), 1.9597(20), 2.1768(23), 1.7110(22),$ and $0.7376(17)$ K. At all fields, our calculations yield $T_{\text{LRO}} > T_{\text{BKT}}$, thus supporting the experimental phenomenology, as can be seen in Fig. 1. We also determined the saturation field to be 17.5 T, in excellent agreement with the experimental value. As in the experiment, the strong dependence of the numerically determined T_{LRO} on the field strength reflects the effect of the field-induced anisotropy. The quantitative differences to the experimental transition temperatures at elevated fields might be resolved by extending the complexity of the modelling. In Fig. S4 of the SM, we obtain a simple estimate of an effective exchange anisotropy $\Delta(H)$ at $H \leq 6$ T and compare it to the low-field results [52].

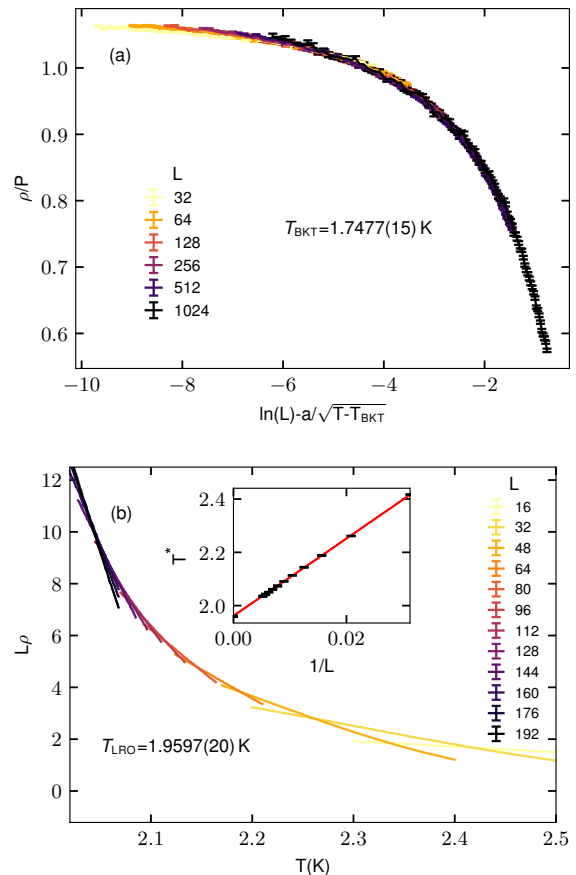


Figure 3. Finite-size scaling analysis performed to obtain the critical temperatures T_{BKT} and T_{LRO} from the QMC simulations at 2 T. (a) Data collapse of the finite-size in-plane spin stiffness ρ fit closely above T_{BKT} , for the $J' = 0$ model, which should collapse to a single curve if the fit is perfect, reaffirming the calculated T_{BKT} . The different curves correspond to different linear sizes L . (b) Crossings of the $L\rho$ curves for the $J' = 1$ mK model; the inset shows the $L \rightarrow \infty$ scaling of the crossing temperature T^* . The red line denotes a second-order polynomial fit, which is extrapolated to $1/L \rightarrow 0$ to estimate T_{LRO} .

Our findings suggest the following scenario for the temperature evolution of spin correlations in CuPOF in applied magnetic fields. Decreasing the temperatures from the paramagnetic high-temperature limit, isotropic Heisenberg-type spin correlations develop which cross over to an anisotropic XY -type close to T_{co} . With further decreasing temperature, the correlation length ξ grows exponentially due to the vortex physics described by BKT theory. For $T \gtrsim T_{\text{BKT}}$, a rather low density of these topological excitations is expected [57]. The exponential increase of ξ yields a rapid strengthening of the antiferromagnetic correlations in the XY regime and, therefore, the staggered magnetization appears effectively non-zero even above T_{LRO} (see SM) [52]. With further increase of ξ upon lowering the temperature further, the mag-

netic correlations, due to the influence of the small but nonzero interlayer interaction J' on the regions with large in-plane correlation lengths, can no longer be treated as 2D, and a transition to long-range order occurs at T_{LRO} . As a consequence of the field-induced BKT-type spin correlations, a concomitant nonmonotonic behavior of the transition temperature T_{LRO} is observed experimentally and confirmed by our QMC simulations.

In conclusion, we found that CuPOF is an experimentally accessible realization of a quasi-2D spin-1/2 Heisenberg square-lattice system with field-tunable magnetic correlations, ranging from almost isotropic Heisenberg to highly-anisotropic XY type. The phenomenology in CuPOF is driven by field-induced Berezinskii-Kosterlitz-Thouless physics under the influence of extremely small interplane interactions, thus providing an attractive opportunity for systematic investigations of the BKT-type topological excitations and calling for further experimental studies by inelastic scattering techniques.

ACKNOWLEDGMENTS

We acknowledge the support of HLD at HZDR, member of the European Magnetic Field Laboratory (EMFL). This work was supported by the Deutsche Forschungsgemeinschaft (DFG) through SFB 1143 (project ID 247310070), the Würzburg-Dresden Cluster of Excellence on Complexity and Topology in Quantum Matter – *ct.qmat* (EXC 2147, project ID 39085490) and the cluster of excellence ML4Q (EXC2004, project ID 390534769). Our QMC code is based on the ALPS libraries [58]. Part of this work was carried out at the STFC ISIS facility and we are grateful for provision of beamtime. This work is supported by EPSRC (UK). For the purpose of open access, the authors have applied a Creative Commons Attribution (CC BY) licence to any Author Accepted Manuscript version arising. Data presented in this paper resulting from the UK effort is available from [59].

AUTHOR CONTRIBUTIONS

D. Opherden and M. S. J. Tepaske contributed equally to this work.

* Corresponding author. E-mail: h.kuehne@hzdr.de

- [1] L. Onsager, Phys. Rev. **65**, 117 (1944).
- [2] N. D. Mermin and H. Wagner, Phys. Rev. Lett. **17**, 1133 (1966).
- [3] L. J. d. Jongh (ed.), Magnetic Properties of Layered Transition Metal Compounds (Springer Netherlands, 1990).
- [4] B. Widom, J. Chem. Phys. **43**, 3898 (1965).

- [5] M. E. Fisher, Rev. Mod. Phys. **46**, 597 (1974).
- [6] K. G. Wilson, Rev. Mod. Phys. **47**, 773 (1975).
- [7] M. J. Feigenbaum, Physica D **7**, 16 (1983).
- [8] P. W. Anderson, Science **235**, 1196 (1987).
- [9] V. L. Berezinskii, J. Exp. Theor. Phys. **32**, 493 (1971).
- [10] J. M. Kosterlitz and D. J. Thouless, J. Phys. C: Solid State Phys. **6**, 1181 (1973).
- [11] J. M. Kosterlitz, J. Phys. Condens. Matter **7**, 1046 (1974).
- [12] B.-G. Liu, Phys. Rev. B **41**, 9563 (1990).
- [13] N. Majlis, S. Selzer, and G. C. Strinati, Phys. Rev. B **45**, 7872 (1992).
- [14] N. Majlis, S. Selzer, and G. C. Strinati, Phys. Rev. B **48**, 957 (1993).
- [15] L. Siurakshina, D. Ihle, and R. Hayn, Phys. Rev. B **61**, 14601 (2000).
- [16] H.-Q. Ding, Phys. Rev. Lett. **68**, 1927 (1992).
- [17] H.-Q. Ding, J. Phys.: Condens. Matter **2**, 7979 (1990).
- [18] A. Cuccoli, T. Roscilde, R. Vaia, and P. Verrucchi, Phys. Rev. Lett. **90**, 167205 (2003).
- [19] B. J. Suh, F. Borsa, L. L. Miller, M. Corti, D. C. Johnston, and D. R. Torgeson, Phys. Rev. Lett. **75**, 2212 (1995).
- [20] D. Waibel, G. Fischer, T. Wolf, H. v. Löhneysen, and B. Pilawa, Phys. Rev. B **91**, 214412 (2015).
- [21] E. S. Klyushina, J. Reuther, L. Weber, A. T. M. N. Islam, J. S. Lord, B. Klemke, M. Månsson, S. Wessel, and B. Lake, Phys. Rev. B **104**, 064402 (2021).
- [22] N. Caci, L. Weber, and S. Wessel, Phys. Rev. B **104**, 155139 (2021).
- [23] A. Cuccoli, T. Roscilde, R. Vaia, and P. Verrucchi, Phys. Rev. B **68**, 060402(R) (2003).
- [24] D. Opherden, N. Nizar, K. Richardson, J. C. Monroe, M. M. Turnbull, M. Polson, S. Vela, W. J. A. Blackmore, P. A. Goddard, J. Singleton, E. S. Choi, F. Xiao, R. C. Williams, T. Lancaster, F. L. Pratt, S. J. Blundell, Y. Skourski, M. Uhlarz, A. N. Ponomaryov, S. A. Zvyagin, J. Wosnitza, M. Baenitz, I. Heinmaa, R. Stern, H. Kühne, and C. P. Landee, Phys. Rev. B **102**, 064431 (2020).
- [25] F. M. Woodward, P. J. Gibson, G. B. Jameson, C. P. Landee, M. M. Turnbull, and R. D. Willett, Inorg. Chem. **46**, 4256 (2007).
- [26] P. A. Goddard, J. Singleton, P. Sengupta, R. D. McDonald, T. Lancaster, S. J. Blundell, F. L. Pratt, S. Cox, N. Harrison, J. L. Manson, H. I. Southerland, and J. A. Schlueter, New J. Phys. **10**, 083025 (2008).
- [27] F. Xiao, F. M. Woodward, C. P. Landee, M. M. Turnbull, C. Mielke, N. Harrison, T. Lancaster, S. J. Blundell, P. J. Baker, P. Babkevich, and F. L. Pratt, Phys. Rev. B **79**, 134412 (2009).
- [28] J. L. Manson, K. H. Stone, H. I. Southerland, T. Lancaster, A. J. Steele, S. J. Blundell, F. L. Pratt, P. J. Baker, R. D. McDonald, P. Sengupta, J. Singleton, P. A. Goddard, C. Lee, M.-H. Whangbo, M. M. Warter, C. H. Mielke, and P. W. Stephens, J. Am. Chem. Soc. **131**, 4590 (2009).
- [29] E. Čížmár, S. A. Zvyagin, R. Beyer, M. Uhlarz, M. Ozerov, Y. Skourski, J. L. Manson, J. A. Schlueter, and J. Wosnitza, Phys. Rev. B **81**, 064422 (2010).
- [30] A. J. Steele, T. Lancaster, S. J. Blundell, P. J. Baker, F. L. Pratt, C. Baines, M. M. Conner, H. I. Southerland, J. L. Manson, and J. A. Schlueter, Phys. Rev. B **84**, 064412 (2011).

- [31] Y. Kohama, M. Jaime, O. E. Ayala-Valenzuela, R. D. McDonald, E. D. Mun, J. F. Corbey, and J. L. Manson, *Phys. Rev. B* **84**, 184402 (2011).
- [32] P. A. Goddard, J. L. Manson, J. Singleton, I. Franke, T. Lancaster, A. J. Steele, S. J. Blundell, C. Baines, F. L. Pratt, R. D. McDonald, O. E. Ayala-Valenzuela, J. F. Corbey, H. I. Southerland, P. Sengupta, and J. A. Schlueter, *Phys. Rev. Lett.* **108**, 077208 (2012).
- [33] P. A. Goddard, J. Singleton, I. Franke, J. S. Möller, T. Lancaster, A. J. Steele, C. V. Topping, S. J. Blundell, F. L. Pratt, C. Baines, J. Bendix, R. D. McDonald, J. Brambleby, M. R. Lees, S. H. Lapidus, P. W. Stephens, B. W. Twamley, M. M. Conner, K. Funk, J. F. Corbey, H. E. Tran, J. A. Schlueter, and J. L. Manson, *Phys. Rev. B* **93**, 094430 (2016).
- [34] V. Selmani, C. P. Landee, M. M. Turnbull, J. L. Wikaira, and F. Xiao, *Inorganic Chemistry Communications* **13**, 1399 (2010).
- [35] P. Sengupta, C. D. Batista, R. D. McDonald, S. Cox, J. Singleton, L. Huang, T. P. Papageorgiou, O. Ignatchik, T. Herrmannsdörfer, J. L. Manson, J. A. Schlueter, K. A. Funk, and J. Wosnitzer, *Phys. Rev. B* **79**, 060409(R) (2009).
- [36] N. A. Fortune, S. T. Hannahs, C. P. Landee, M. M. Turnbull, and F. Xiao, *J. Phys. Conf. Ser.* **568**, 042004 (2014).
- [37] P. Sengupta, A. W. Sandvik, and R. R. P. Singh, *Phys. Rev. B* **68**, 094423 (2003).
- [38] D. Opherden, F. Bärthel, S. Yamamoto, Z. T. Zhang, S. Luther, S. Molatta, J. Wosnitzer, M. Baenitz, I. Heinmaa, R. Stern, C. P. Landee, and H. Kühne, *Phys. Rev. B* **103**, 014428 (2021).
- [39] H.-Q. Ding and M. S. Makivić, *Phys. Rev. Lett.* **64**, 1449 (1990).
- [40] F. Borsa, M. Corti, T. Goto, A. Rigamonti, D. C. Johnston, and F. C. Chou, *Phys. Rev. B* **45**, 5756 (1992).
- [41] F. Tabak, A. Lascialfari, and A. Rigamonti, *J. Phys.: Condens. Matter* **5**, B31 (1993).
- [42] L. Bossoni, P. Carretta, R. Nath, M. Moscardini, M. Baenitz, and C. Geibel, *Phys. Rev. B* **83**, 014412 (2011).
- [43] P. Gaveau, J. P. Boucher, L. P. Regnault, and Y. Henry, *J. Appl. Phys.* **69**, 6228 (1991).
- [44] P. C. Hohenberg and B. I. Halperin, *Rev. Mod. Phys.* **49**, 435 (1977).
- [45] M. Campostrini, M. Hasenbusch, A. Pelissetto, P. Rossi, and E. Vicari, *Physical Rev. B* **65**, 144520 (2002).
- [46] A. W. Sandvik, *Phys. Rev. Lett.* **80**, 5196 (1998).
- [47] D. R. Nelson and J. M. Kosterlitz, *Phys. Rev. Lett.* **39**, 1201 (1977).
- [48] M. S. Makivić, *Phys. Rev. B* **46**, 3167 (1992).
- [49] H.-Q. Ding, *Phys. Rev. B* **45**, 230 (1992).
- [50] We note that a constant was added in the fits to account for the paramagnetic contribution to $1/T_1$.
- [51] A. Cuccoli, T. Roscilde, V. Tognetti, R. Vaia, and P. Verrucchi, *Phys. Rev. B* **67**, 104414 (2003).
- [52] See Supplemental Material at (link will be inserted by publisher) for additional information about the staggered spin correlations investigated by means of NMR, μ^+ SR, and QMC, as well as an estimate of the field-induced exchange anisotropy, which includes Refs [60–65].
- [53] O. F. Syljuåsen and A. W. Sandvik, *Phys. Rev. E* **66**, 046701 (2002).
- [54] Y.-D. Hsieh, Y.-J. Kao, and A. W. Sandvik, *J. Stat. Mech.: Theory Exp.* P09001 (2013).
- [55] A. W. Sandvik, *Aip Conference Proceedings* **1297**, 135 (2010).
- [56] D. J. Luitz, F. Alet, and N. Laflorencie, *Phys. Rev. B* **89**, 165106 (2014).
- [57] K. Yosida, *Theory of Magnetism* (Springer-Verlag, Berlin and Heidelberg, 1996).
- [58] B. Bauer, L. D. Carr, H. G. Evertz, A. Feiguin, J. Freire, S. Fuchs, L. Gamper, J. Gukelberger, E. Gull, S. Guertler, A. Hehn, R. Igarashi, S. V. Isakov, D. Koop, P. N. Ma, P. Mates, H. Matsuo, O. Parcollet, G. Pawłowski, J. D. Picon, L. Pollet, E. Santos, V. W. Scarola, U. Schollwöck, C. Silva, B. Surer, S. Todo, S. Trebst, M. Troyer, M. L. Wall, P. Werner, and S. Wessel, *Journal of Statistical Mechanics: Theory and Experiment* P05001 (2011).
- [59] <https://wrap.warwick.ac.uk/139957>
- [60] J. Als-Nielsen, S. T. Bramwell, M. T. Hutchings, G. J. McIntyre, and D. Visser, *J. Phys.: Condens. Matter* **5**, 7871 (1993).
- [61] S. V. Isakov and R. Moessner, *Phys. Rev. B* **68**, 104409 (2003).
- [62] S. T. Bramwell and P. C. W. Holdsworth, *J. Phys.: Condens. Matter* **5**, L53 (1993).
- [63] S. T. Bramwell and P. C. W. Holdsworth, *Phys. Rev. B* **49**, 8811 (1994).
- [64] A. Taroni, S. T. Bramwell, and P. C. W. Holdsworth, *J. Phys.: Condens. Matter* **20**, 275233 (2008).
- [65] M. Troyer, M. Imada, and K. Ueda, *J. Phys. Soc. Jpn.* **66**, 2957 (1997).

Supplemental Material: Field-tunable Berezinskii-Kosterlitz-Thouless correlations in a Heisenberg magnet

D. Opherden,¹ M. S. J. Tepaske,^{2,3} F. Bärtl,^{1,4} M. Weber,³ M. M. Turnbull,⁵ T. Lancaster,⁶ S. J. Blundell,⁷ M. Baenitz,⁸ J. Wosnitzer,^{1,4} C. P. Landee,⁹ R. Moessner,³ D. J. Luitz,^{2,3} and H. Kühne^{1,*}

¹*Hochfeld-Magnetlabor Dresden (HLD-EMFL) and Würzburg-Dresden Cluster of Excellence ct.qmat, Helmholtz-Zentrum Dresden-Rossendorf, 01328 Dresden, Germany*

²*Physikalisches Institut, Universität Bonn, Nussallee 12, 53115 Bonn, Germany*

³*Max Planck Institute for the Physics of Complex Systems, 01187 Dresden, Germany*

⁴*Institut für Festkörper- und Materialphysik, TU Dresden, 01062 Dresden, Germany*

⁵*Carlson School of Chemistry, Clark University, Worcester, MA 01610, USA*

⁶*Durham University, Centre for Materials Physics, South Road, Durham DH1 3LE, UK*

⁷*Clarendon Laboratory, Department of Physics, University of Oxford, Park Road, Oxford OX1 3PU, UK*

⁸*Max Planck Institute for Chemical Physics of Solids, 01187 Dresden, Germany*

⁹*Department of Physics, Clark University, Worcester, MA 01610, USA*

(Dated: September 23, 2022)

Staggered spin correlations probed by NMR and μ^+ SR

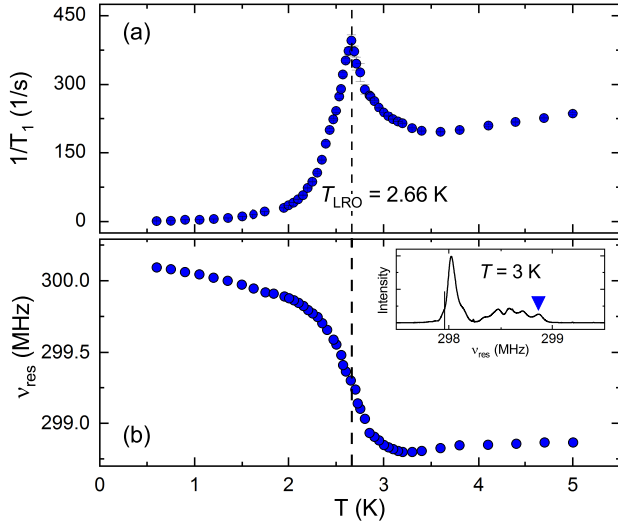


Figure S1. Temperature-dependent ^1H -NMR (a) spin-lattice relaxation rate and (b) resonance frequency of CuPOF at 7 T. The vertical dashed line indicates the transition temperature $T_{\text{LRO}} = 2.66$ K. A representative ^1H -NMR spectrum at 3 K is shown in the inset of (b). The blue triangle marks the spectral line under investigation. The solid vertical line indicates the Larmor frequency $\nu_{\text{L}} = 297.96$ MHz, given by the external field.

In order to investigate the effect of the field-tunable XY anisotropy on the quasi-static spin correlations, we probed the evolution of the staggered magnetization as an effective order parameter. As reported previously, the ^1H -NMR spectra of CuPOF yield a distinct line splitting at low temperatures, which provides a direct probe of the local staggered magnetization [1]. More precisely, the NMR spectrum represents a histogram of the quasi-static fields, probed at the positions of the resonantly

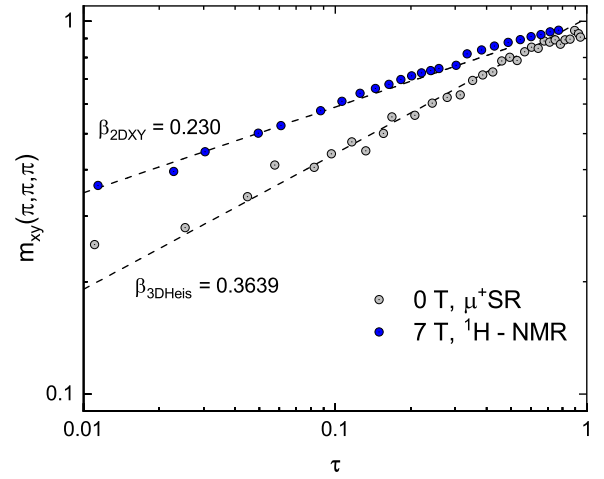


Figure S2. Log-log plot of the normalized ^1H -NMR and μ^+ SR frequencies (μ^+ SR data are from Ref. [1]), probing the staggered magnetization $m_{xy}(\pi, \pi, \pi)$, and plotted as a function of the reduced temperature $\tau = 1 - T/T_c$, with $T_c = T_{\text{LRO}}$. The dashed lines are plots of $m_{xy} \propto \tau^\beta$, where β denotes an effective critical exponent.

excited nuclear moments, on the time scale of the measuring process (a few ten μs here). The temperature-dependent resonance frequency ν_{res} (determined as the first spectral moment) of a line at the high-frequency end of the ^1H -NMR spectrum, recorded at 7 T, is presented in Fig. S1(b). The corresponding ^1H nuclear spin-lattice relaxation rate is presented in Fig. S1(a), and yields $T_{\text{LRO}} = 2.66$ K, identical to T_{LRO} as determined from the ^{31}P spin-lattice relaxation rate, see Fig. 2(b) in the main text. A deviation of ν_{res} from an almost constant value at high temperatures occurs at about 3 K $\simeq T_{\text{co}} > T_{\text{LRO}}$.

Whereas the staggered magnetization already becomes non-zero in the XY regime, we define the maximum temperature of the ^1H spin-lattice relaxation rate as critical temperature, see Fig. S1(a), as supported by the

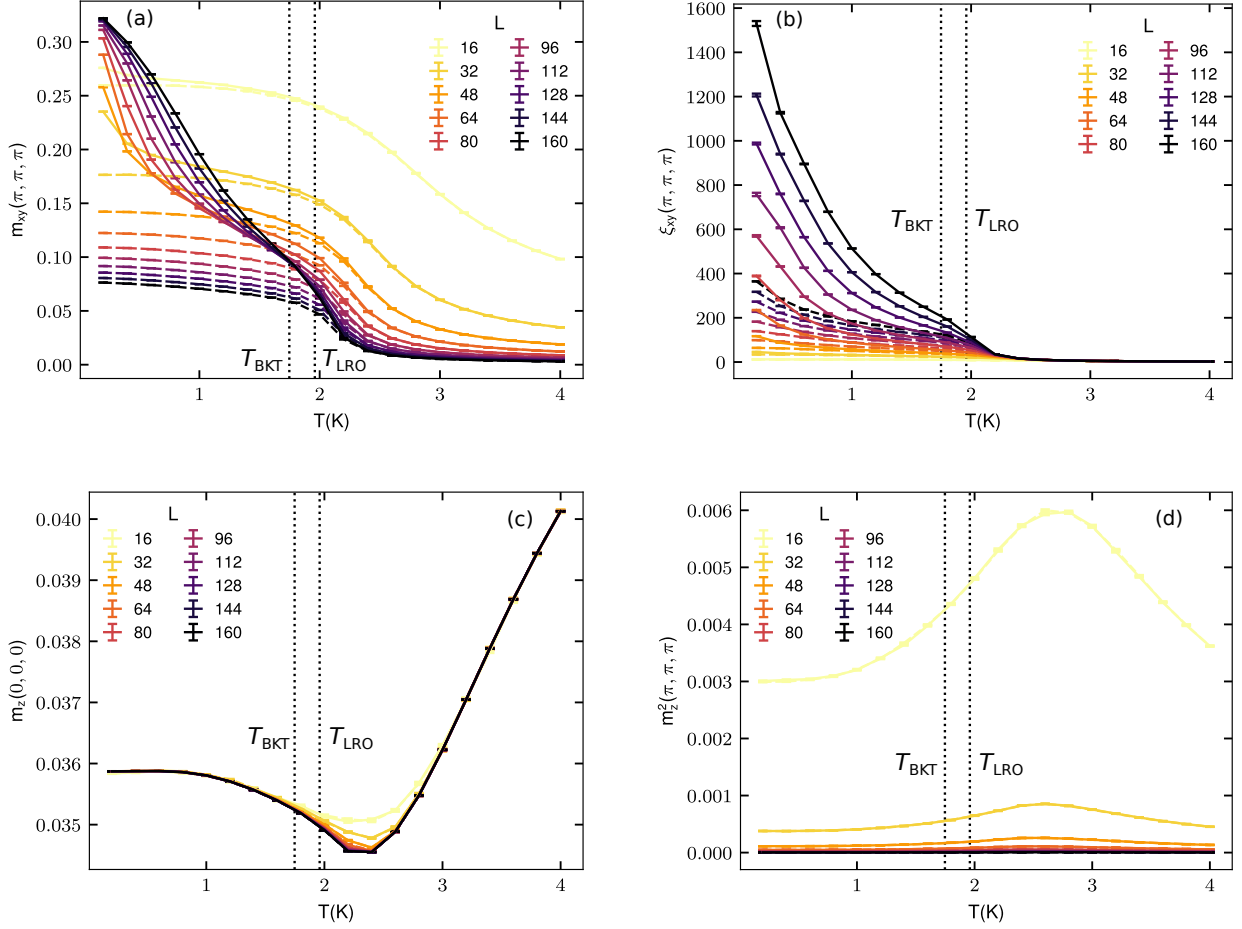


Figure S3. (a) The staggered in-plane magnetization $m_{xy}(\pi, \pi, \pi)$, (b) the corresponding correlation length $\xi_{xy}(\pi, \pi, \pi)$, (c) the uniform out-of-plane magnetization $m_z(0, 0, 0)$, and (d) the squared staggered out-of-plane magnetization $m_z^2(\pi, \pi, \pi)$, all determined from the structure factor. The lattices have sizes $L \times L \times L/8$ and we simulated the Hamiltonian (1) in the main text with intralayer coupling $J/k_B = 6.8$ K, interlayer coupling $J'/k_B = 1$ mK, intrinsic exchange anisotropy $\Delta = 0.0185$, and magnetic field strength $\mu_0 H = 2$ T. The solid lines are for the $J' = 1$ mK model and the dashed lines for $J' = 0$. The vertical dashed lines denote the critical temperatures T_{BKT} and T_{LRO} as determined in Fig. 3 in the main text.

following reasoning. In a layered anisotropic magnetic lattice, the correlation length significantly increases with decreasing temperature, following an exponential growth described as $\xi_{2\text{DXY}} \propto \exp(0.5\pi/\sqrt{T/T_{\text{BKT}} - 1})$ [2, 3]. In the presence of a finite interlayer coupling J' , the transition to long-range order is expected at $\xi^2 J'/J \simeq 1$ [4]. According to our QMC simulations, at T_{LRO} , the in-plane correlation length is of the order of 100 lattice spacings, as can be seen for $\mu_0 H = 2$ T in Fig. S3(b). With $J'/J \simeq 1.4 \times 10^{-4}$ for CuPOF [1], the condition $\xi^2 J'/J \simeq 1$ is satisfied at T_{LRO} .

Closely below T_c , the staggered magnetization $m_{xy}(\pi, \pi, \pi)$ scales with the reduced temperature $\tau = (1 - T/T_c)$ as $m_{xy} \propto \tau^\beta$, where β may be interpreted as an effective critical exponent. Here, we study to what extent the expected universality classes of an (an)isotropic spin system in (non-)zero field are reflected in the exper-

imental data, but note that there may in practise be a broad crossover region “interpolating” between the two (Heisenberg and XY) cases [5].

Employing $T_c = T_{\text{LRO}} = 2.66$ K at 7 T, we plot the normalized ^1H resonance frequency as a function of the reduced temperature in a log-log plot, see Fig. S2. We find a good agreement when comparing with the critical exponent $\beta_{2\text{DXY}} = 3\pi^2/128 \simeq 0.23$ of a finite-size 2D XY model [6, 7]. Similar observations were made for other materials that realize a planar XY lattice [8, 9]. The same analysis was applied to the $\mu^+\text{SR}$ frequency at zero field [1], using $T_c = 1.38(2)$ K, giving a good agreement when comparing to the critical exponent $\beta_{3\text{DHeis}} = 0.3639(35)$ [10] of the 3D Heisenberg model, and, similarly well, to the critical exponent $\beta_{3\text{DXY}} = 0.33$ [4] of the 3D XY model. These observations further support the scenario of the enhanced anisotropy of intralayer

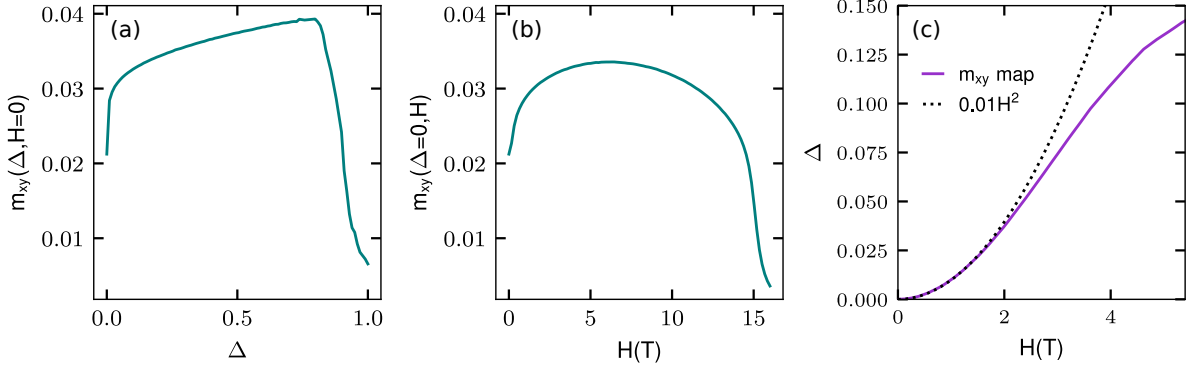


Figure S4. (a) The staggered in-plane magnetizations $m_{xy}(\Delta, H = 0)$ and (b) $m_{xy}(\Delta = 0, H)$ for an $L \times L = 100 \times 100$ Heisenberg system at $T = 1.2$ K. In (c), we show the numerically determined field-induced exchange anisotropy $\Delta(H)$, that was determined for $\mu_0 H \leq 6$ T by solving $m_{xy}(\Delta, H = 0) = m_{xy}(\Delta = 0, H)$. The black dotted line shows the quadratic dependence with $\Delta = 0.01(\mu_0 H)^2$.

spin correlations at elevated fields.

Staggered spin correlations calculated with QMC

To infer the pattern of the long-range order that is associated to T_{LRO} , which was calculated with QMC by examining the $L\rho$ crossings in the lower panel of Fig. 3 in the main text, we also calculate the in-plane structure factor S_{xy} and the corresponding correlation length ξ [11], i.e.,

$$S_{xy}(\vec{k}) = \sum_j e^{i\vec{k}\cdot\vec{r}_j} (\langle S_0^x S_j^x \rangle + \langle S_0^y S_j^y \rangle), \quad (1)$$

$$\xi_{xy}(\vec{k}) = \frac{L}{2\pi} \sqrt{\frac{S_{xy}(\vec{k})}{S_{xy}(\vec{k} + \vec{d}\vec{k})} - 1}. \quad (2)$$

Here, we introduced a staggering phase based on the lattice position \vec{r}_j of site j and a staggering vector \vec{k} with nearest-by vector $\vec{k} + \vec{d}\vec{k}$. This structure factor can be used to define a magnetization via $m_{xy}^2 = S_{xy}(\vec{k})/N$, where N denotes the amount of spins. In Fig. S3(a), we show the staggered in-plane magnetization $m_{xy}(\pi, \pi, \pi)$ at 2 T as a function of temperature for various values of L , and in Fig. S3(b) we show the corresponding correlation length $\xi_{xy}(\pi, \pi, \pi)$. The $J' = 1$ mK results are shown as solid lines and the $J' = 0$ results as dashed lines. We see an onset of the magnetization and in-plane spin-correlations at T_{LRO} that does not scale to zero with system size when J' is nonzero.

In Fig. S3(c), we show the uniform out-of-plane magnetization $m_z(0, 0, 0)$, which depicts the field dependency of the out-of-plane canting of the in-plane antiferromagnetic order and converges with system size. To verify that the magnetic order is only in-plane staggered, we show the squared staggered out-of-plane magnetization

$m_z(\pi, \pi, \pi)$ in Fig. S3(d), which clearly scales to zero for large system sizes.

Field-induced exchange anisotropy

As a simple estimate of the field-induced exchange anisotropy, we compute the staggered in-plane magnetizations $m_{xy}(\Delta, H = 0)$ and $m_{xy}(\Delta = 0, H)$ for an $L \times L = 100 \times 100$ Heisenberg system at $T = 1.2$ K, and find $\Delta(H)$ such that $m_{xy}(\Delta, H = 0) = m_{xy}(\Delta = 0, H)$ is satisfied. This condition should hold if the Hamiltonians $\mathcal{H}(\Delta, H = 0)$ and $\mathcal{H}(\Delta = 0, H)$ can be mapped onto each other, thereby giving an estimate of the field-induced exchange anisotropy $\Delta(H)$. In Figs. S4(a) and S4(b), we show $m_{xy}(\Delta, H = 0)$ and $m_{xy}(\Delta = 0, H)$, and in Fig. S4(c) we show the numerically determined field-induced exchange anisotropy $\Delta(H)$ that was found at $H \leq 6$ T. To compare with the perturbative quadratic field dependence estimate from [12], we also plot the quadratic curve $\Delta = 0.01(\mu_0 H)^2$, showing excellent agreement at small H .

* Corresponding author. E-mail: h.kuehne@hzdr.de

- [1] D. Opherden, N. Nizar, K. Richardson, J. C. Monroe, M. M. Turnbull, M. Polson, S. Vela, W. J. A. Blackmore, P. A. Goddard, J. Singleton, E. S. Choi, F. Xiao, R. C. Williams, T. Lancaster, F. L. Pratt, S. J. Blundell, Y. Skourski, M. Uhlarz, A. N. Ponomaryov, S. A. Zvyagin, J. Wosnitza, M. Baenitz, I. Heinmaa, R. Stern, H. Kühne, and C. P. Landee, Phys. Rev. B **102**, 064431 (2020).
- [2] J. M. Kosterlitz, J. Phys. Condens. Matter **7**, 1046 (1974).
- [3] H.-Q. Ding, Phys. Rev. Lett. **68**, 1927 (1992).

- [4] J. Als-Nielsen, S. T. Bramwell, M. T. Hutchings, G. J. McIntyre, and D. Visser, *J. Phys.: Condens. Matter* **5**, 7871 (1993).
- [5] S. V. Isakov and R. Moessner, *Phys. Rev. B* **68**, 104409 (2003).
- [6] S. T. Bramwell and P. C. W. Holdsworth, *J. Phys.: Condens. Matter* **5**, L53 (1993).
- [7] S. T. Bramwell and P. C. W. Holdsworth, *Phys. Rev. B* **49**, 8811 (1994).
- [8] A. Taroni, S. T. Bramwell, and P. C. W. Holdsworth, *J. Phys.: Condens. Matter* **20**, 275233 (2008).
- [9] E. S. Klyushina, J. Reuther, L. Weber, A. T. M. N. Islam, J. S. Lord, B. Klemke, M. Månsson, S. Wessel, and B. Lake, *Phys. Rev. B* **104**, 064402 (2021).
- [10] M. Troyer, M. Imada, and K. Ueda, *J. Phys. Soc. Jpn.* **66**, 2957 (1997).
- [11] A. W. Sandvik, *Aip Conference Proceedings* **1297**, 135 (2010).
- [12] P. Sengupta, C. D. Batista, R. D. McDonald, S. Cox, J. Singleton, L. Huang, T. P. Papageorgiou, O. Ignatchik, T. Herrmannsdörfer, J. L. Manson, J. A. Schlueter, K. A. Funk, and J. Wosnitza, *Phys. Rev. B* **79**, 060409(R) (2009).